Original Research Article

Improved Cerebellar Structure and Neuronal Restoration by Combined Extracts of Ginger, Garlic, and Turmeric in Lead-Exposed Rats: A Histological and Morphometric Study

Abstract

Background: Heavy metal toxicity, particularly from lead exposure, poses significant neurodevelopmental risks, with the cerebellum being a key target. This study evaluated the ameliorative potential of a phytobiotic formulation comprising aqueous extracts of *Zingiber officinale* (ginger), *Allium sativum* (garlic), and *Curcuma longa* (turmeric) on lead-induced cerebellar damage in Wistar rats.

Methods: Twenty-five (25) adult male Wistar rats were randomly assigned into five groups (n = 5). Lead neurotoxicity was induced via oral administration of lead acetate (150 mg/kg/day) for 14 days. Groups 3–5 received combined phytobiotic extracts at 300, 400, and 500 mg/kg body weight, respectively, co-administered with lead acetate. Group 6 received phytobiotics alone. Extracts were prepared by aqueous maceration of authenticated plant materials, concentrated by evaporation, and administered via oral gavage. Following treatment, cerebellar tissues were harvested, fixed in 10% buffered formalin, and processed for hematoxylin and eosin (H\&E) staining. Morphometric analysis of Purkinje cell count and morphology was conducted using ImageJ software. Statistical analysis was performed using one-way ANOVA with Tukey's post hoc test (SPSS v26).

Results: Lead exposure resulted in significant loss and shrinkage of Purkinje cells, cortical disorganization, and reduced cell count ($p < 0.05$). Co-administration of the phytobiotic formulation, particularly at moderate and high doses, markedly preserved cerebellar cytoarchitecture and significantly improved Purkinje cell density and morphology ($p < 0.05$) compared to the lead-only group.

Conclusion: The aqueous phytobiotic mixture of ginger, garlic, and turmeric confers dose-dependent neuroprotection against lead-induced cerebellar damage, likely due to their synergistic antioxidant and anti-inflammatory properties. These findings support their therapeutic potential in environmental neurotoxicity.

Keywords: Lead acetate, Cerebellum, Phytobiotics, *Zingiber officinale*, *Curcuma longa*, *Allium sativum*, Purkinje cells, Neuroprotection

Commented [gk1]: N=5 or 6 Group 6 received phytobiotics alone and con negative not mention here ????

Commented [gk2]: Mention the period (for .....)

1. Introduction

Heavy metal pollution remains a major environmental and public health challenge worldwide, with lead (Pb) being one of the most prevalent and toxic contaminants. Lead exposure occurs through various sources including industrial emissions, contaminated water, soil, paints, and food (Jaishankar et al., 2014). Once in the body, lead accumulates in soft tissues and bones, crossing the blood-brain barrier to exert profound neurotoxic effects, particularly on the developing nervous system (Flora et al., 2012). The cerebellum, responsible for motor coordination and balance, is highly vulnerable to oxidative damage

Commented [gk3]: How that in 2026

caused by lead due to its high lipid content and oxygen consumption (Zhou et al., 2026). Mechanistically, lead induces oxidative stress, disrupts neurotransmitter release, interferes with calcium homeostasis, and damages neuronal integrity, resulting in long-term neurobehavioral deficits (Virgolini & Aschner, 2021).

Although chelation therapy remains the conventional treatment for lead toxicity, it is often associated with adverse effects, high costs, and limited efficacy, particularly in reversing neuronal damage (Gracia & Snodgrass, 2007). Consequently, there is growing interest in exploring safer and more affordable alternative therapies, particularly phytochemicals with antioxidant and neuroprotective properties.

Among such natural agents, *Curcuma longa* (turmeric), *Zingiber officinale* (ginger), and *Allium sativum* (garlic) have received considerable attention. These plants are rich in bioactive compounds such as curcumin (from turmeric), gingerol and shogaol (from ginger), and allicin and organosulfur compounds (from garlic), which exhibit potent antioxidant, anti-inflammatory, antimicrobial, and neuroprotective activities (Ajanaku et al., 2022; Dilip et al., 2021).

Studies have demonstrated the individual benefits of these botanicals in combating oxidative stress and heavy metal-induced damage. For instance, Sudjarwo et al. (2017) reported that curcumin significantly ameliorated lead acetate-induced testicular toxicity in rats by enhancing antioxidant defense mechanisms and reducing lipid peroxidation. Similarly, Abubakar et al. (2019) demonstrated that curcumin protected against Pb-induced cerebellar neurotoxicity by attenuating oxidative stress and chelating free lead ions. The phytochemicals in ginger and garlic have also shown promise against bacterial pathogens and oxidative injury. Awan et al. (2017), using phytochemical and FT-IR analysis, confirmed that extracts of *Z. officinale* and *A. sativum* possess significant antibacterial properties and may offer cost-effective means of managing disease and combating antimicrobial resistance.

Moreover, the application of phytobiotics in animal nutrition has yielded promising results in aquaculture. Kusi et al. (2025) evaluated the dietary supplementation of *C. longa*, *A. sativum*, and *Z. officinale* in Nile tilapia (*Oreochromis niloticus*) and found enhanced growth performance, feed utilization, and resistance to *Streptococcus agalactiae* infection. These findings suggest a potential for the synergistic use of these botanicals in improving systemic health and resilience to environmental stressors, including infections and toxicants.

Despite these promising findings, there remains a significant gap in the literature regarding the combined effect of aqueous extracts of these three plants on the nervous system, particularly the cerebellum, under lead-induced oxidative stress. Most existing studies have examined the effects of individual extracts or focused on organs such as the liver, kidneys, and testes (Flora et al., 2012; Sudjarwo et al., 2017). The cerebellum, being a critical hub for motor control and cognition, deserves focused investigation, especially under heavy metal exposure scenarios.

Furthermore, there is limited quantitative histological data—such as neuronal cell counts, mean cell size, area percentage, and intensity of staining—supporting the neuroprotective claims of these phytochemicals. Histomorphometric analysis using Hematoxylin and Eosin (H\&E) staining, alongside image-based quantification, provides critical insights into tissue architecture and cellular integrity in neurotoxicological studies.

Therefore, this study seeks to fill this knowledge gap by investigating the protective effects of combined aqueous extracts of *Z. officinale, A. sativum, and C. longa* on Pb-induced cerebellar damage in Wistar rats. It evaluates not only the general histopathological features but also employs morphometric assessments to objectively quantify neuronal preservation. By elucidating the neuroprotective potential of this phytochemical combination, this research aims to contribute to the development of effective, affordable, and accessible interventions for managing lead neurotoxicity.

2. Materials and Methods

2.1. Experimental Animals

Twenty-five adult Wistar rats (weighing 150–200 g) were used in this study. The animals were obtained from the Animal House of the Faculty of Basic Medical Sciences, University of Calabar, and acclimatized for one week under standard laboratory conditions (temperature 22–26°C, 12 h light/dark cycle) with free access to food and water. All animal handling procedures were conducted in accordance with guidelines nof the Faculty Animal Research Ethics Committee (FAREC-FBMS), Faculty of Basic Medical Science, University of Calabar, Calabar with an issued number: 312ANA5821.

Commented [gk4]: Correct

2.2. **Identification of Plants and Chemicals**

Commented [gk5]: You must mention the weight of each material use in the extract and the concentration after extract .

Aqueous extracts of *Zingiber officinale*, *Allium sativum*, and *Curcuma longa* were prepared using standardized procedures involving drying, pulverizing, and decoction in distilled water, followed by filtration and concentration (Krakowska-Sieprawska et al., 2022). Matured rhizomes of *Zingiber officinale* and *Curcuma longa*, as well as mature bulbs of *Allium sativum*, were sourced from Watt Market in Calabar, located in Cross River State. These plant materials were identified by a taxonomist from the Department of Botany, Faculty of Biological Sciences, University of Calabar. Voucher numbers assigned to each specimen are as follows: Bot/Herb/UCC/179 for *Allium sativum*, Bot/Herb/UCC/178 for *Zingiber officinale*, and Bot/Herb/UCC/177 for *Curcuma longa.*

Commented [gk6]: Need to prepare freshly because it lost the active materials after short time , you use it for 14 day ???

Additionally, approximately 50 grams of lead acetate was obtained, weighed, and purchased from the Department of Pure and Applied Chemistry, Faculty of Physical Sciences, University of Calabar. The chemical was supplied by Archit Meta Chem, Ahmedabad-380004, Gujarat, India, with CAS number 301-04-2.

Commented [gk7]: Mention how to prepare dissolve in ..... and concentration and dose

2.3. Experimental Design

The rats were randomly divided into five (5) groups (n = 5 per group):

Commented [gk8]: In abstract you mention a group 6 received phytobiotics alone where is it correct the number of g

Group A (Negative Control): Received distilled water only.
Group B (Positive Control): Received lead acetate (150 mg/kg/day, orally) for 14 days.
Group C (Low Dose Treatment): Received lead acetate (150 mg/kg/day) for 14 days, then co-administered 300 mg/kg of each extract for 14 days.
Group D (Moderate Dose Treatment): Received lead acetate (150 mg/kg/day) for 14 days, then 400 mg/kg of each extract for 14 days.
Group E (High Dose Treatment): Received lead acetate (150 mg/kg/day) for 14 days, then 500 mg/kg of each extract for 14 days.

2.4. Anesthesia and Euthanasia

Animals were anesthetized with an intraperitoneal injection of ketamine (80 mg/kg) prior to sacrifice to harvest the brain tissues.

2.5. Tissue Processing and Histological Analysis

Brain tissues were dissected and fixed in 10% neutral-buffered formalin for 48 hours. Standard paraffin-embedding techniques were followed. Sections of 5 µm thickness were obtained using a rotary microtome and stained with Hematoxylin and Eosin (H\&E) using established protocols (Cardiff et al., 2014).

2.6. Microscopy and Image Analysis

Photomicrographs of the cerebellar sections were taken at ×400 magnification using a light microscope fitted with a digital camera. The images were calibrated using a micrometer scale and analyzed using ImageJ software (NIH, USA) for the following parameters:

Cell count (n): Manual or semi-automated counting of stained neuronal cell bodies within defined regions of interest (ROIs).

Total area (µm²): Area covered by neuronal profiles within the ROI, determined via thresholding and segmentation tools.

Average cell size (µm²): Calculated by dividing total area by the number of counted cells.

Percentage area (% ROI)' Proportion of the field occupied by neurons relative to the total field area.

Intensity values (mean gray value): Reflecting the average pixel intensity of neuronal structures to assess staining density.

2. Parameter Quantification:

For each image, the following parameters were evaluated:

Each measurement was repeated in multiple fields per animal (minimum of 3–5 ROIs), and the mean value was used for statistical analysis.

7. Statistical Analysis

All data were expressed as mean ± standard deviation (SD). Statistical comparisons among groups were performed using **one-way ANOVA followed by Tukey's post hoc test for multiple comparisons using IBM SPSS version 25.0.

3. Results

3.1 Histological Observations

Following a 14-day experimental period, histological analysis of cerebellar tissue stained with hematoxylin and eosin (H\&E) and examined at 400× magnification revealed the following observations across the experimental groups:

Group A (Negative Control)

Cerebellar sections from the negative control group, which did not receive either lead acetate or plant extracts, exhibited normal histoarchitecture. The molecular (M), Purkinje (P), and granular (G) layers were clearly delineated and well preserved. Numerous intact Purkinje neurons were prominently observed at the interface between the molecular and granular layers (Figure 1; Plate 1).

Group B (Positive Control/Lead Acetate)

Sections from the group treated with 150 mg/kg body weight of lead acetate for 14 days displayed significant histological alterations. There was notable degeneration of Purkinje cells, with prominent vacuolations within the Purkinje cell layer and the granular layer. The Purkinje cells appeared sparse and structurally compromised (Figure 1; Plate 2).

Group C (Low Dose Treatment)

Tissues from the group that received lead acetate followed by treatment with 300 mg/kg body weight of each aqueous extract of *Zingiber officinale*, *Allium sativum*, and *Curcuma longa* showed moderate architectural disruption. Degenerating Purkinje neurons and marked vacuolations were evident in both the Purkinje and granular layers (Figure 1; Plate 3).

Group D (Moderate Dose Treatment)

Cerebellar sections from animals treated with 400 mg/kg of each plant extract following lead exposure revealed improved cytoarchitecture compared to the low-dose group. However, mild vacuolations persisted within the Purkinje cell layer, and fewer Purkinje neurons were observed (Figure 1; Plate 4).

Group E (High Dose Treatment)

The group administered 500 mg/kg of each extract post-lead exposure exhibited significant histological recovery. The cerebellar layers—molecular, Purkinje, and granular—appeared distinct and intact. Numerous healthy Purkinje neurons were evident, indicating a dose-dependent neuroprotective effect of the extracts (Figure 1; Plate 5).

Plate 1-5: Photomicrographs of H&E-Stained Cerebellar Sections from Experimental Groups at ×400 Magnification

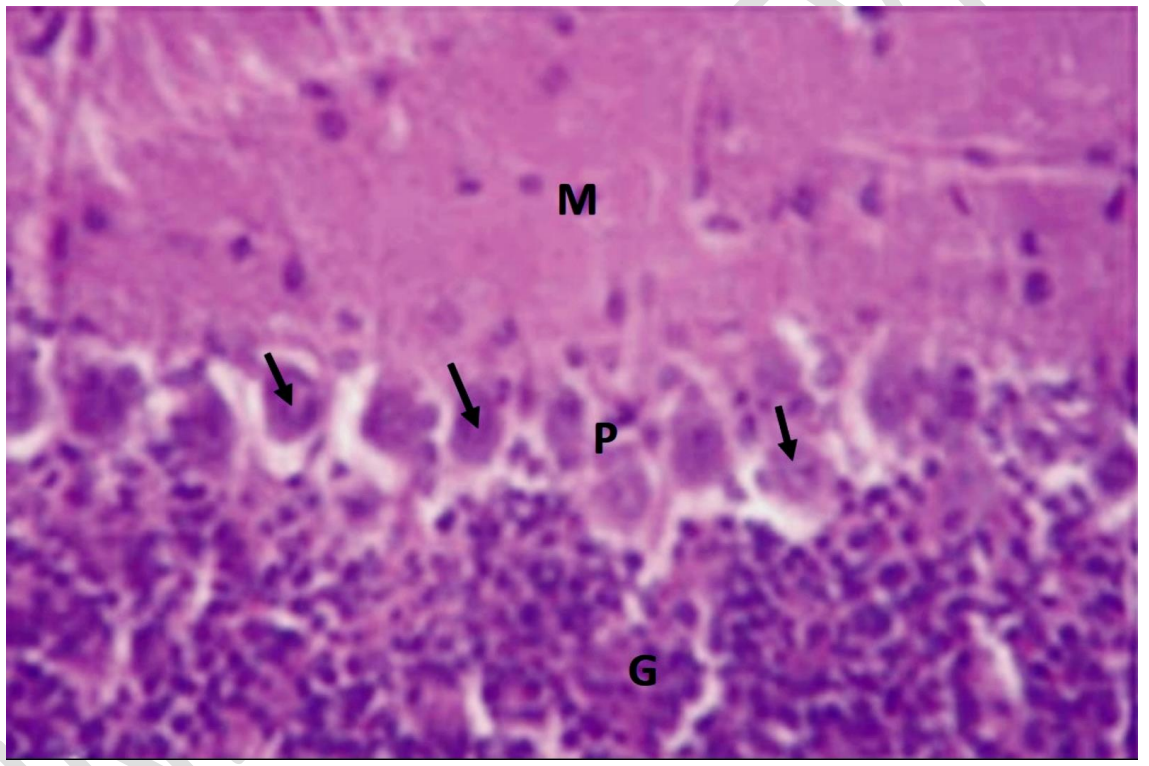

Commented [gk9]: Replace the picture with another with high resolution

Commented [gk10]: Delete . you mention it in the end of caption

PLATE 1: Photomicrograph of the cerebellum – Group A (Negative Control)

Hematoxylin and eosin (H\&E) stained section showing well-preserved cerebellar cytoarchitecture. The molecular layer (M), Purkinje cell layer (P), and granular layer (G) appear clearly defined and intact. Numerous normal Purkinje neurons are visible at the junction between the molecular and granular layers. *(H\&E, ×400)*

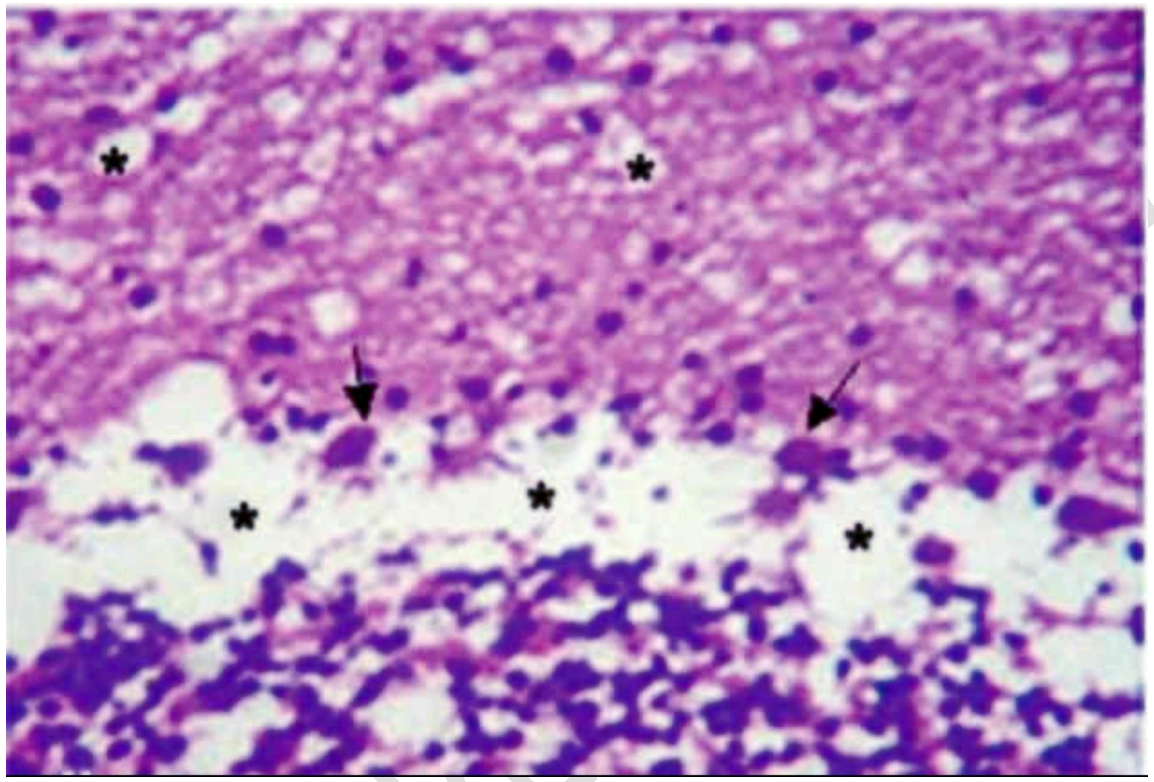

Commented [gk11]: This is a Neuronophagia is the process where damaged or dying neurons are engulfed and removed by phagocytic cells, primarily microglia, within the central nervous system.
Not depletion and degeneration

Commented [gk12]: Add the marks in the pictures to the caption

PLATE 2: Photomicrograph of the cerebellum – Group B (Positive Control/Lead Acetate)

Section showing cerebellar architecture following administration of lead acetate (150 mg/kg). There is marked depletion and degeneration of Purkinje neurons, with extensive vacuolations in both the Purkinje and granular layers. The Purkinje cell population appears reduced and scattered. *(H\&E, ×400)*

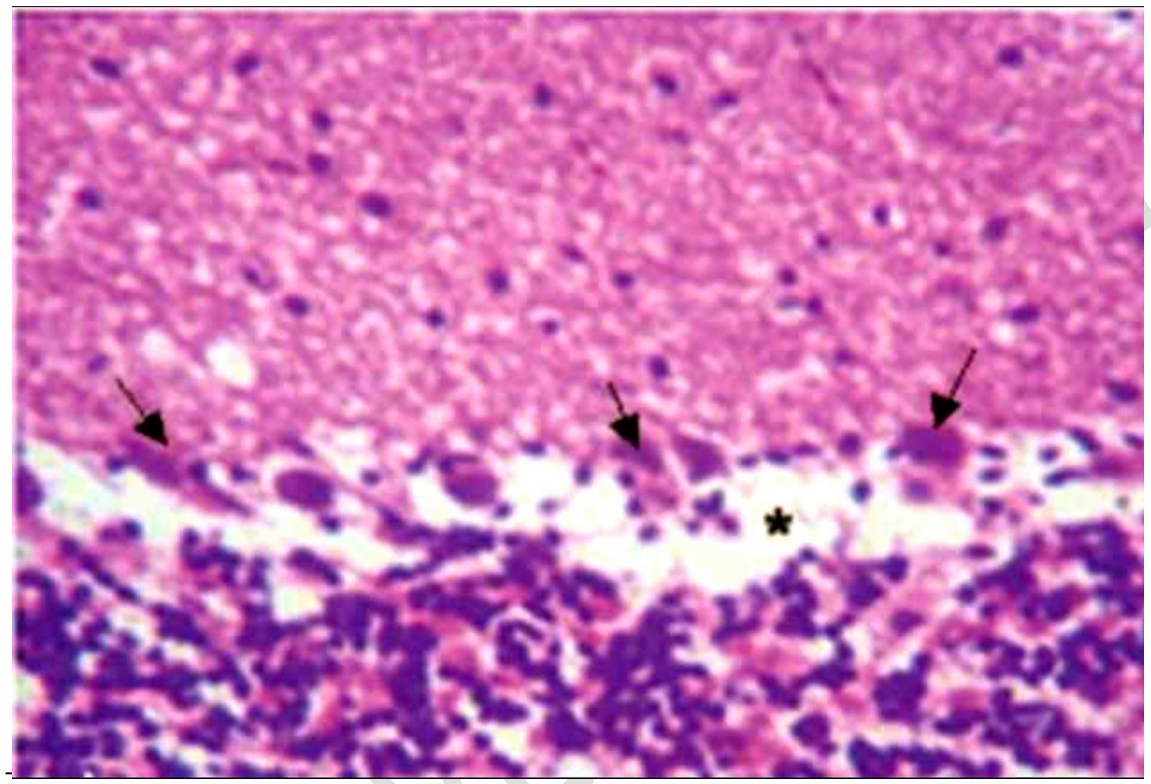

PLATE 3: Photomicrograph of the cerebellum – Group C (Low Dose Treatment)

Cerebellar section from rats exposed to lead acetate followed by treatment with low-dose aqueous extracts (300 mg/kg each of *Zingiber officinale, Allium sativum, and Curcuma longa*). Moderate cytoarchitectural distortion and neuronal degeneration are evident, with vacuolations within the Purkinje and granular layers. *(H\&E, ×400)*

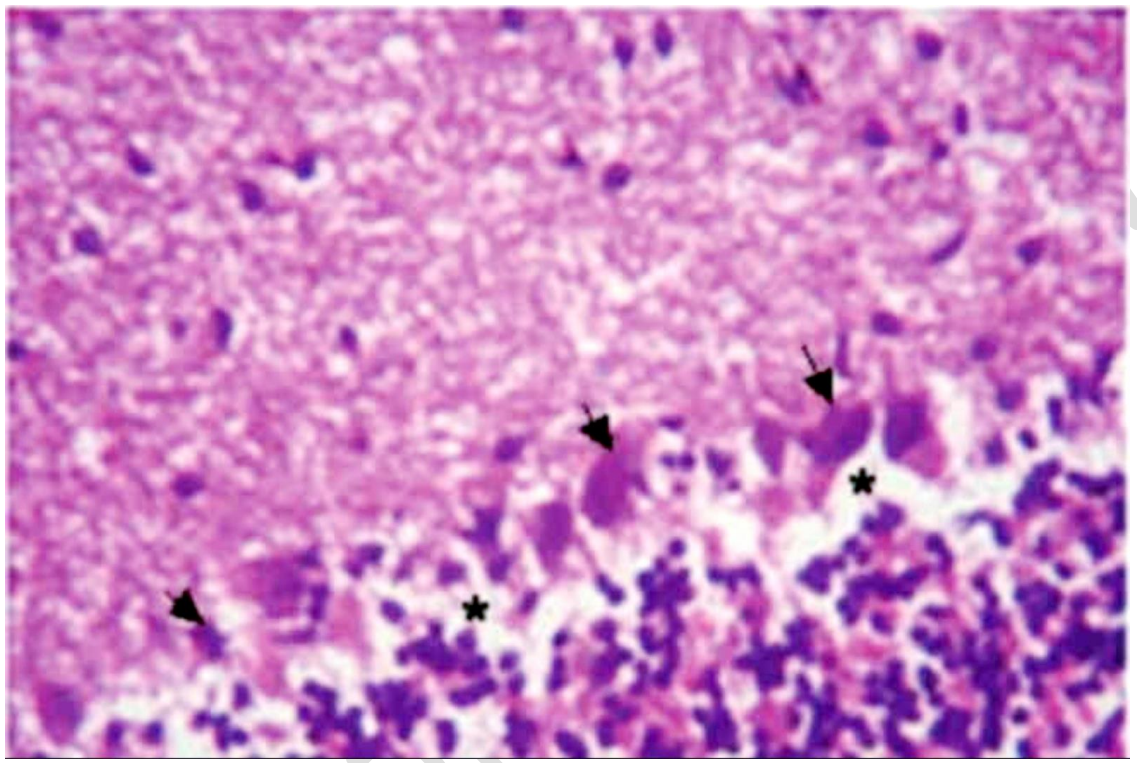

PLATE 4: Photomicrograph of the cerebellum – Group D (Moderate Dose Treatment)

Section showing cerebellar tissue post-lead exposure and moderate-dose extract treatment (400 mg/kg of each plant extract). Fewer Purkinje cells are observed, with mild to moderate vacuolation in the Purkinje layer, indicating partial neuroprotection. *(H\&E, ×400)*

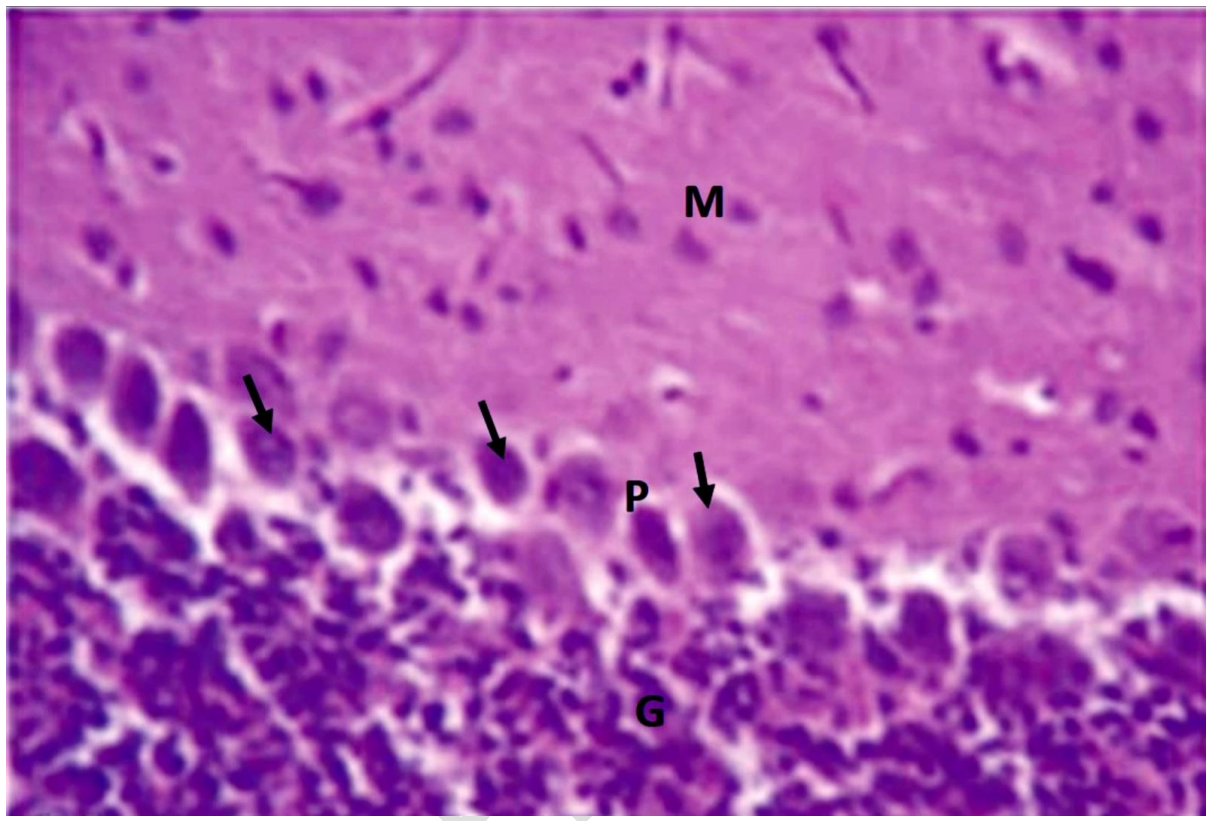

PLATE 5: Photomicrograph of the cerebellum – Group E (High Dose Treatment)

H\&E-stained section showing nearly normal cerebellar architecture in rats treated with high-dose plant extracts (500 mg/kg each) after lead exposure. The molecular (M), Purkinje (P), and granular (G) layers are well defined, with prominent and intact Purkinje neurons, suggesting effective histological recovery. *(H\&E, ×400)*

3.2 Morphometric Evaluation of Cerebellar Neurons Using ImageJ Analysis

The morphometric data extracted using ImageJ from cerebellar sections stained with hematoxylin and eosin (H\&E) demonstrate significant alterations across experimental groups:

The negative control group exhibited the highest cell count (110.00 ± 2.00), larger total measured area (14,480.00 ± 86.59 µm²), and highest percentage area occupied by cells (32.83%), indicating intact cerebellar architecture.

In contrast, the positive control group (lead acetate only) showed marked reductions in all parameters: cell count (55.00 ± 3.00), total area (6,450.00 ± 63.41 µm²), and area percentage (17.70%), reflecting severe cellular loss and tissue damage.

Treatment groups (low, moderate, and high dose) showed a dose-dependent improvement in all histomorphometric indices. The high dose group showed near-complete restoration:

Cell count: 104.00 ± 2.00

Total area: 14,055.67 ± 136.26 µm²

Area percentage: 30.73%

Similarly, average cell size and staining intensity (pixel value) followed a restorative trend in treated groups, with the high dose group values approaching those of the negative control.

Table 1: Morphometric Parameters of H&E-Stained Cerebellar Sections Analyzed at ×400 Magnification Using ImageJ

Group	Cell Count (Mean ± SD)	Total Area Measured (µm²)	Average Size (µm²)	Area %	Intensity Value (0–255)
Negative Control	110.00 ± 2.00	14874.00 ± 77.38	135.23 ± 3.00	32.83 ± 0.31	145.00 ± 1.00
Positive Control/Lead	55.00 ±	6450.00 ±	117.50 ±	17.70 ±	122.00 ±

Acetate	3.00*	63.41*	5.37	0.56*	2.00*
Low Dose	66.33 ± 2.52*a	7932.00 ± 80.29*a	119.67 ± 3.30 *	21.20 ± 0.36*a	131.67 ± 1.53*a
Moderate Dose	74.00 ± 2.00*a	9485.00 ± 85.00*ab	128.20 ± 4.23	26.20 ± 0.76*ab	138.00 ± 1.00*b
High Doseabc	104.00 ± 2.00abc	14055.67 ± 136.26*abc	135.20 ± 1.42b	30.73 ± 0.65abc	143.33 ± 0.58abc
Total (All Groups)	81.87 ± 22.32	10559.33 ± 3458.30	127.16 ± 8.36	25.73 ± 5.89	136.00 ± 8.78

Note: All values are expressed as Mean ± Standard Deviation (SD).

Figure 1: Cerebellar Cell Count Across Experimental Groups Following Lead Exposure and Treatment

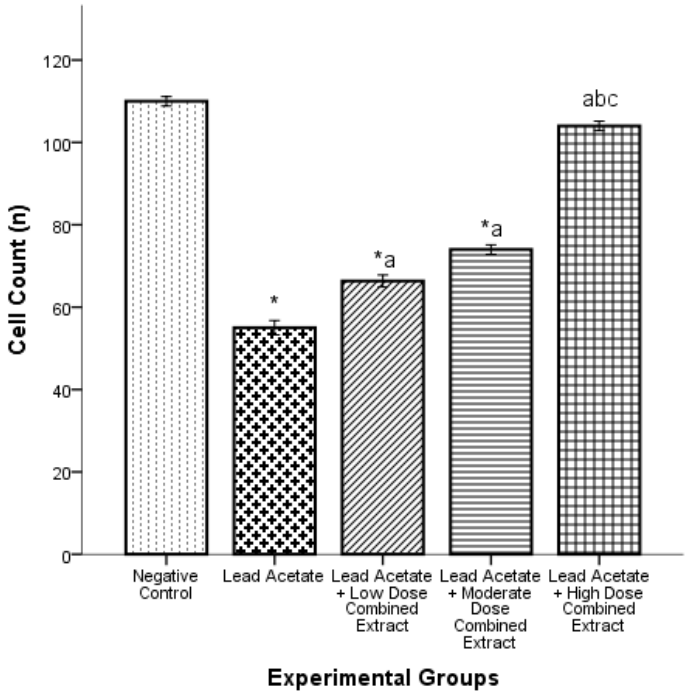

Bar chart showing the mean number of neurons per region of interest in H&E-stained cerebellar sections analyzed at ×400 magnification using ImageJ. A significant decrease was observed in the positive control group compared to the negative control, while treatment groups showed dose-dependent restoration. Data are expressed as Mean ± SD; $p < 0.05$ indicates significant difference from negative control, a from lead acetate, b from low dose, c from moderate dose.

Figure 2: Comparison of Total Neuronal Area in H&E-Stained Cerebellar Tissue Following Treatments

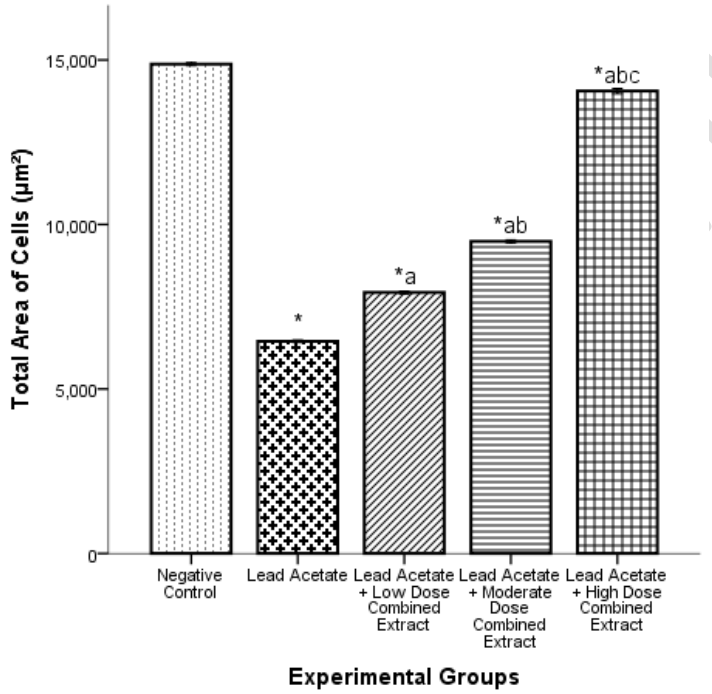

This figure depicts the total region (µm²) occupied by neuronal structures as assessed via ImageJ in ×400 magnification H&E-stained sections. The positive control group showed reduced area, while increasing doses of the test agent significantly improved the neuronal coverage. Data are expressed as Mean ± SD; statistical notations as described in Fig. 1.

Figure 3: Group-wise Variation in Cerebellar Neuronal Size (µm²)

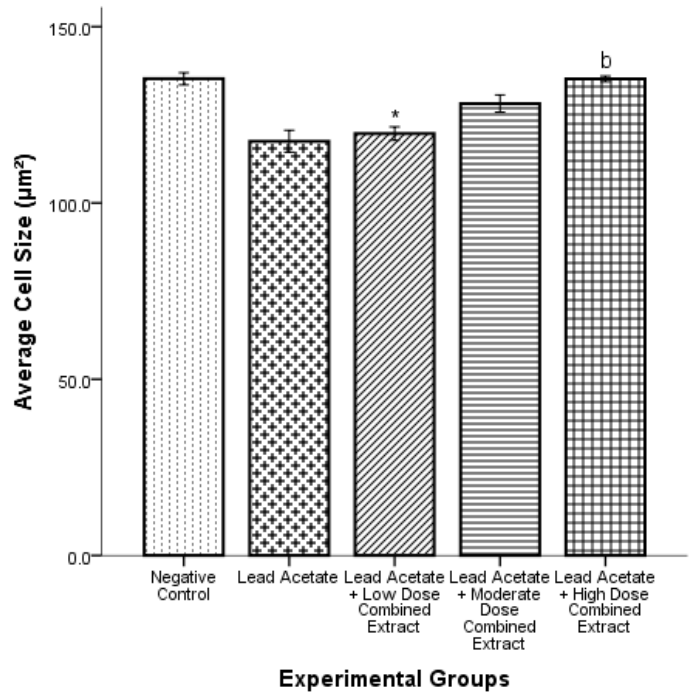

The bar chart illustrates the mean cell size (µm²) calculated from segmented neurons. While the lead-exposed group had slightly reduced sizes, treatment groups—particularly moderate and high doses—approached normal cell dimensions. Mean ± SD; significance indicated as in Fig. 1.

Figure 4: Group-wise Comparison of Total Neuronal Area in the Cerebellum

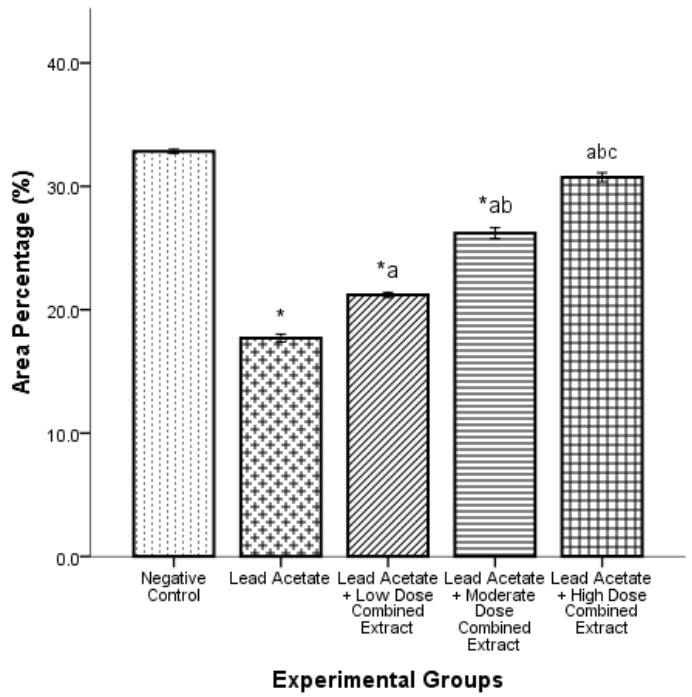

Chart represents the proportion of the ROI (%) occupied by neurons. Lead exposure drastically reduced area %, which was ameliorated in a dose-responsive manner in treated groups. Mean ± SD; $p < 0.05$ compared to control and treatment differences as denoted in Fig. 1.

Figure 5: Comparative Mean Pixel Intensity of Neurons in the Cerebellum

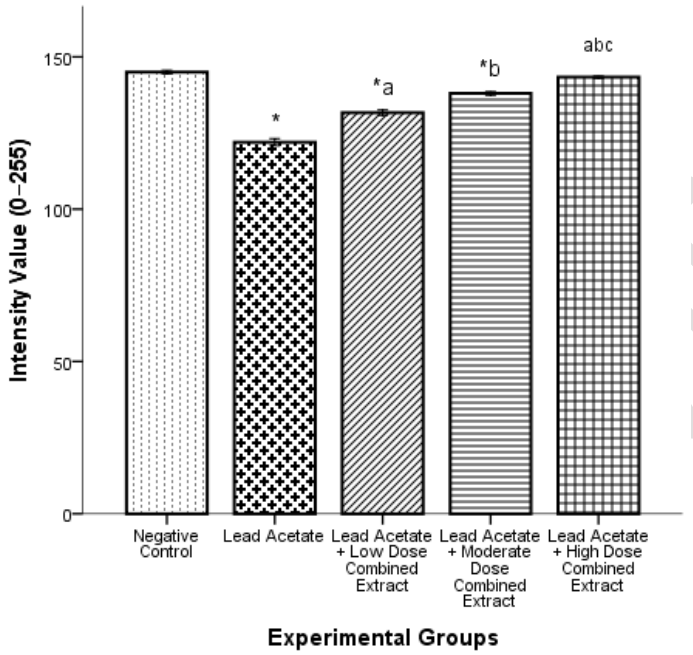

This figure shows pixel intensity (0–255 grayscale) reflecting the staining density of neuronal regions in the cerebellum. Lower intensity values in the positive control indicate weaker staining, while treatment improved staining uniformity. Data are expressed as Mean ± SD; statistical indicators follow the same notation as in preceding figures.
Average signal intensity within cells in the cerebellum

4. Discussion

This study investigated the neuroprotective potential of combined aqueous extracts of *Zingiber officinale*, *Allium sativum*, and *Curcuma longa* against lead acetate-induced cerebellar toxicity in Wistar rats, using both qualitative histopathology and quantitative morphometric analysis. The findings revealed that lead exposure (150 mg/kg body weight) induced significant neurodegeneration in the cerebellum, characterized by the loss and degeneration of Purkinje cells, vacuolations within the granular and Purkinje layers, and distortion of the overall cerebellar cytoarchitecture. These observations are consistent with previous reports on the neurotoxic effects of lead, which include oxidative stress, mitochondrial dysfunction, apoptosis, and structural derangement in brain regions involved in motor control (Alqahtani & Albasher, 2021, Ayinla & Asuku, 2025; Zhang et al., 2022; Chao et al., 2007, Amedu & Omotoso, 2020).

In the current study, the negative control group exhibited normal cerebellar architecture, with intact molecular, Purkinje, and granular layers, and well-defined Purkinje neurons—serving as a baseline for comparison. In contrast, the positive control group (Pb-only) presented extensive histological damage and a marked reduction in all morphometric parameters, including cell count, neuronal area, area percentage, average size, and staining intensity. This reflects the toxic impact of lead acetate on neuronal structure, likely mediated through mechanisms such as increased lipid peroxidation, disruption of calcium homeostasis, and inhibition of antioxidant enzymes (Sanders et al., 2009; Abubakar et al., 2019).

However, treatment with combined aqueous extracts of ginger, garlic, and turmeric at graded doses (300, 400, and 500 mg/kg each) conferred dose-dependent neuroprotection. The low-dose group showed moderate improvement with partial restoration of cerebellar layers and Purkinje neurons. The moderate-dose group revealed fewer vacuolations and better cellular preservation. The high-dose group, notably, demonstrated near-complete restoration of histoarchitecture, with clearly delineated layers and numerous intact Purkinje neurons—approaching the normalcy observed in the negative control.

These results are corroborated by the morphometric findings. The cell count, total neuronal area, and area percentage in the high-dose group were significantly higher than in the Pb-only group and comparable to the control. Average neuronal size and pixel intensity, indicators of structural integrity and staining affinity, also followed a restorative trend, suggesting improvement in cell viability and preservation of proteinaceous content (Gupta et al., 2013; Christian et al., 2017).

The therapeutic effects observed in this study may be attributed to the phytochemical synergy among the three extracts. *Curcuma longa* (turmeric) contains curcumin, a potent antioxidant and metal chelator, known to reduce Pb accumulation and ameliorate oxidative damage in neural tissues (Sudjarwo et al., 2017; Abubakar et al., 2019). *Zingiber officinale* (ginger) is rich in gingerols, shogaols, and flavonoids, which possess anti-inflammatory and antioxidant activities that mitigate neural inflammation and apoptosis (Christian et al., 2017). *Allium sativum* (garlic) contains organosulfur compounds (e.g., allicin) and selenium that enhance endogenous antioxidant systems and inhibit lipid peroxidation, reducing Pb-induced cytotoxicity (Uzma et al., 2017).

Together, these bioactive components likely acted synergistically to reduce oxidative stress, scavenge free radicals, stabilize neuronal membranes, and chelate lead ions, thereby mitigating neurodegeneration. The dose-response relationship observed further supports the therapeutic potential of phytochemical combinations, especially in chronic or subacute toxicological conditions.

While the findings are promising, several limitations warrant consideration. The study used only male rats, hence sex-specific variations in neurotoxicity and treatment response were not assessed. Biochemical assays of oxidative stress markers (e.g., SOD, MDA, GPx) were not conducted alongside histology, which could have strengthened the mechanistic insights. The study duration was relatively short (14 days); longer studies may be needed to assess chronic outcomes or delayed neurodegeneration.

This study adds to the growing evidence supporting the use of phytochemicals as affordable neuroprotectants in heavy metal-induced toxicity. Given the widespread environmental exposure to lead—especially in developing countries—such interventions could serve as preventive or adjunct therapies for at-risk populations.

5. Conclusion

The present study demonstrates that **combined aqueous extracts of *Zingiber officinale*, *Allium sativum*, and *Curcuma longa*** exhibit **significant neuroprotective effects** against lead-induced cerebellar damage in Wistar rats. These effects were evident both histologically and morphometrically, with the high-dose treatment group showing the **most pronounced restoration of cerebellar architecture and neuronal integrity**. The findings suggest that these commonly available plant-based extracts may offer a **cost-effective and natural therapeutic strategy for mitigating lead-induced neurotoxicity. Further studies are warranted to elucidate the molecular pathways involved and to explore clinical translation.

References

1. Jaishankar, M., Tseten, T., Anbalagan, N., Mathew, B. B., & Beeregowda, K. N. (2014). Toxicity, mechanism and health effects of some heavy metals. *Interdisciplinary Toxicology*, 7(2), 60–72. https://doi.org/10.2478/intox-2014-0009

2. Flora, G., Gupta, D., & Tiwari, A. (2012). Toxicity of lead: A review with recent updates. *Interdisciplinary Toxicology*, *5*(2), 47–58. https://doi.org/10.2478/v10102-012-0009-2

3. Zhou, Y., Sanchez, V. B., Xu, P., Roule, T., Flores-Mendez, M., Ciesielski, B., Yoo, D., Teshome, H., Jimenez, T., Liu, S., Henne, M., O'Brien, T., He, Y., Mesaros, C., Tobalu, F. O., & Enogieru, A. B. (2025). Lead neurotoxicity in experimental models: A systematic review on effects on the cerebrum, cerebellum, and hippocampus. *Toxicology Reports*, *14*, 102044. https://doi.org/10.1016/j.toxrep.2025.102044

4. Virgolini, M. B., & Aschner, M. (2021). Molecular mechanisms of lead neurotoxicity. *Advances in Neurotoxicology*, *5*, 159–213. https://doi.org/10.1016/bs.ant.2020.11.002

5. Gracia, R. C., & Snodgrass, W. R. (2007). Lead toxicity and chelation therapy. *American Journal of Health-System Pharmacy*, *64*(1), 45–53. https://doi.org/10.2146/ajhp060175

6. Ajanaku, C. O., Ademosun, O. T., Atohengbe, P. O., Ajayi, S. O., Obafemi, Y. D., Owolabi, O. A., Akinduti, P. A., & Ajanaku, K. O. (2022). Functional bioactive compounds in ginger, turmeric, and garlic. *Frontiers in Nutrition*, *9*, 1012023. https://doi.org/10.3389/fnut.2022.1012023

7. Chowdhury, D. K., Sahu, N. P., Sardar, P., Deo, A. D., Bedekar, M. K., Singha, K. P., & Maiti, M. K. (2021). Feeding turmeric in combination with ginger or garlic enhances the digestive enzyme activities, growth and immunity in *Labeo rohita* fingerlings. *Animal Feed Science and Technology*, *277*, 114964. https://doi.org/10.1016/j.anifeedsci.2021.114964

8. Sudjarwo, S. A., Sudjarwo, G. W., & Koerniasari. (2017). Protective effect of curcumin on lead acetate-induced testicular toxicity in Wistar rats. *Research in Pharmaceutical Sciences, 12*(5), 381–390. https://doi.org/10.4103/1735-5362.213983

9. Abubakar, K., Muhammad Mailafiya, M., Danmaigoro, A., Musa Chiroma, S., Abdul Rahim, E. B., & Abu Bakar Zakaria, M. Z. (2019). Curcumin attenuates lead-induced cerebellar toxicity in rats via chelating activity and inhibition of oxidative stress. *Biomolecules, 9*(9), 453. https://doi.org/10.3390/biom9090453

10. Awan, U. A., Ali, S., Shahnawaz, A. M., Shafique, I., Zafar, A., Khan, M. A. R., Ghous, T., Saleem, A., & Andleeb, S. (2017). Biological activities of *Allium sativum* and *Zingiber officinale* extracts on clinically important bacterial pathogens, their phytochemical and FT-IR spectroscopic analysis. *Pakistan Journal of Pharmaceutical Sciences, 30*(3), 729–745.

11. Kusi, I., Obirikorang, K. A., & Adjei-Boateng, D. (2025). Effects of phytobiotic Curcuma longa, *Allium sativum*, and *Zingiber officinale*-supplemented diets on growth, utilization of feed, and Nile tilapia (*Oreochromis niloticus*) resistance against *Streptococcus agalactiae*. *Aquaculture Research.* Advance online publication. https://doi.org/10.1155/are/9911375

12. Krakowska-Sieprawska, A., Kiełbasa, A., Rafińska, K., Ligor, M., & Buszewski, B. (2022). Modern methods of pre-treatment of plant material for the extraction of bioactive compounds. *Molecules, 27*(3), 730. https://doi.org/10.3390/molecules27030730

13. Cardiff, R., Miller, C. H., & Munn, R. J. (2014). Manual hematoxylin and eosin staining of mouse tissue sections. *Cold Spring Harbor Protocols, 2014*(6), pdb.prot073411. https://doi.org/10.1101/pdb.prot073411

14. Alqahtani, W. S., & Albasher, G. (2021). Moringa oleifera Lam. extract rescues lead-induced oxidative stress, inflammation, and apoptosis in the rat cerebral cortex. *Journal of Food Biochemistry, 45*(1), e13579. https://doi.org/10.1111/jfbc.13579

15. Ayinla, M. T., & Asuku, O. A. (2025). The neurotoxic effects of lead acetate and the abrogating actions of 6-gingerol-rich extract of ginger via modulation of antioxidant defence system, pro-inflammatory markers, and apoptotic cascade. *Naunyn-Schmiedeberg's Archives of Pharmacology, 398* (7), 9341–9356. https://doi.org/10.1007/s00210-025-03873-x

16. Zhang, J., Su, P., Xue, C., Wang, D., Zhao, F., Shen, X., & Luo, W. (2022). Lead disrupts mitochondrial morphology and function through induction of ER stress in models of neurotoxicity. *International Journal of Molecular Sciences, 23*(19), 11435. https://doi.org/10.3390/ijms231911435

17. Chao, S. L., Moss, J. M., & Harry, G. J. (2007). Lead-induced alterations of apoptosis and neurotrophic factor mRNA in the developing rat cortex, hippocampus, and cerebellum. *Journal of Biochemical and Molecular Toxicology, 21*(5), 265–272. https://doi.org/10.1002/jbt.20191

18. Niu, Y., Zhang, R., Cheng, Y., Sun, X., & Tian, J. (2002). Effect of lead acetate on the apoptosis and the expression of bcl-2 and bax genes in rat brain cells. *Zhonghua Yu Fang Yi Xue Za Zhi, 36*(1), 30–33. PMID: 11955345

19. Amedu, N. O., & Omotoso, G. O. (2020). Lead acetate-induced neurodegenerative changes in the dorsolateral prefrontal cortex of mice: The role of vitexin. *Environmental Analysis, Health & Toxicology, 35*(1), e2020001. https://doi.org/10.5620/eaht.e2020001